Journal Article

Inductive heating effects on friction surfacing of stainless steel onto an aluminium substrate

Stegmueller, M. J. R., Schindele, P. and Grant, R. J.

Recommended citation:
Stegmueller, M. J. R., Schindele, P. and Grant, R. J. (2015), 'Inductive heating effects on friction surfacing of stainless steel onto an aluminium substrate', *Journal of Materials Processing Technology*, Vol.216, pp.430-439. doi: 10.1016/j.jmatprotec.2014.10.013

Inductive heating effects on friction surfacing of stainless steel onto an aluminium substrate

M.J.R. Stegmueller[a,b,*], P. Schindele[a], R.J. Grant[b]

[a]*Kempten University of Applied Sciences, Dept. Mechanical Engineering, Germany*
[b]*Glyndwr University, Dept. Engineering and Applied Physics, Wrexham, United Kingdom LL11 2AW*

Abstract

An experimental setup was designed to compare the principal process parametric relationships with the classical approach to friction surfacing with the addition of inductive heating. The production of the flash is described quantitatively and its influence on coating geometry and mass is presented. It was found that the coating mass and thickness decreased for an increase in the rotational speed of the consumable rod; the amount of flash produced by the consumable rod also increased. However, the effect of an increase in this rod contact pressure on the coating thickness is insignificant, whilst the coating mass decreases with rising pressure and the coating width increases coupled with an increase in flash production. Cross sections showed good bonding quality and mechanical interlocking at the bond interface. The substrate-coating interface showed a varying degree of mechanical interlocking and the presence of cavitations. Bond strength values applying shear and push-off testing of up to 106 MPa and 96 MPa, respectively, could be identified.

Keywords: inductive heating, friction surfacing, parametric study, stainless steel, coating, aluminium, bond strength

1. Introduction

Derived from friction welding a new process was designed which is widely mentioned in literature as friction surfacing. With friction surfacing, the face of a rotating

*Corresponding author
Email addresses: michael.stegmueller@fh-kempten.de (M.J.R. Stegmueller), paul.schindele@fh-kempten.de (P. Schindele), r.j.grant@glyndwr.ac.uk (R.J. Grant)

cylindrical rod is axially pressed against a flat substrate. The rotating consumable rod is then, under the creation of a flash at the face of the rod, moved along the substrate with a defined travel speed producing a coated layer. The process uses frictionally generated heat, which is a function of axial force and rotational speed, for softening the coating material. The process with its parameters and their corresponding relationships was subject to closer investigations over the last twenty years.

Process parameters are the rotational speed and consumption feed rate of the coating rod i.e. the rate at which the consumable rod is being eroded, the applied axial force on the coating rod and the travel speed with which the rod is moved along the substrate.

Vitanov and Voutchkov (2005) presented empirical relationships between the axial force applied to the coating rod, its rotational and travel speed. The aim was to optimize the coating concerning its thickness, width and bond strength with the help of fuzzy rules and membership functions. However, this classical approach to friction surfacing causes problems related to the process itself.

Stern (1996) claims that it is unlikely that hard materials such as steel will coat onto soft substrates such as aluminium because the soft material will deform preferentially. Whereas Chandrasekaran et al. (1997a) claims that stainless steel does not flow as easily as mild steel, during friction surfacing onto an aluminium substrate, which could be related to the difference in hardnesses.

Another problem is the production of a flash during the coating process along with its quantification (Gandra et al. (2014)). The flash is created at the tip of the coating rod where it contacts the substrate. As stated by Hanke et al. (2012), this flash limits the possible coating length because it interferes with the continuity of the coating by contacting the collet chuck of the electric drive in which the coating rod is fixed and consequently the process has to be stopped. Therefore, it is important that the amount of flash material produced is reduced to a minimum.

K Fukakusa (1996) offered a deeper insight into flash production by using two different coating materials within one coating rod to determine the "diameter of the real rotational contact plane" (i.e. the effective rod diameter in contact with the substrate) during coating. The coating materials were prepared by drilling a central hole in one

end of the consumable rod (stainless steel X6Cr13), wherein a tracer material with similar mechanical properties at high temperatures (X5CrNi18-10) was inserted. The diameteral variation of the tracer material showed a borderline where rod material is being either formed as a coating on the substrate or as a flash at the coating rod tip.

The bond strength of the coating can be determined with various methods. The determination of the tensile strength for thermal sprayed coatings by the tensile adhesive test described in DIN EN 582, offers an easy-to-prepare test setup which can be installed in an universal tensile testing machine. However, the application of a metallic adhesive to connect the coating to the push-off body limits the maximum testing load to the tensile strength of the adhesive as presented by Lin and Berndt (1994).

Marot et al. (2006) states that the use of a shear test for thermal sprayed coatings, as defined by DIN 15340, offers the advantage of fast and easy specimen preparation without the disadvantage of a maximum test load inherent in DIN EN 582.

Both DIN tests ensure determination of standardized values, but the mixed mode failure or cohesive failure in either substrate or coating causes distortion of the bond strength value. It should be noted that a certain geometrical shape of the specimens with defined dimensions is required, which for small specimens can present preparation problems.

Two suitable test setups for the determination of the bond strength can be found in the friction surfacing literature. Voutchkov et al. (2001) presented a method in which the specimen can be prepared by drilling a hole from the back side of the substrate until the tool contacts the coating interface. A pin is inserted in the bore and pushes off the coating (Fig. 1). The specimens for this testing method can be prepared accurately and easily with a milling machine.

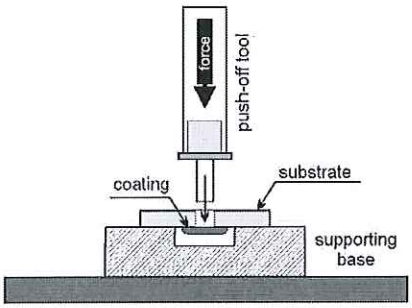

Fig. 1. Push-off test with bore. Voutchkov et al. (2001)

For the determination of the coating-substrate shear strength a tensile testing machine can be used to implement the setup presented by Khalid Rafi et al. (2010) (see Fig. 2). Additionally, the specimens can be quickly prepared by milling to a well defined cross-sectional area.

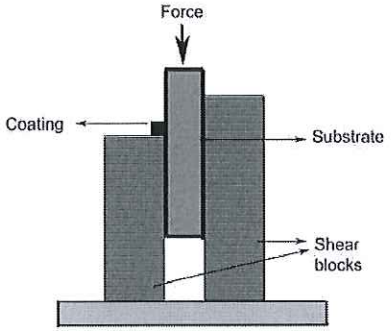

Fig. 2. Shear strength test. Khalid Rafi et al. (2010)

This paper presents investigations of the friction surfacing process behaviour by using an additional heat source to heat the consumable stainless steel rod before and during friction surfacing of an aluminium substrate. The materials were thought suitable for this initial study because Chandrasekaran et al. (1997a) has claimed that the combination forms an inhomogeneously coated layer with no proper bond. Push-off and shear testing was employed as presented by Voutchkov et al. (2001) and Khalid Rafi et al. (2010), respectively, to create comparable bond strength values. This paper addresses

the influence of various parameters on the coating process including:

- coating and flash mass,
- coating thickness and length,
- consumption feed rate of the coating rod,
- and bond strength.

The authors wish to demonstrate that stainless steel can be coated onto aluminium forming a consistently good bond with a minimum of coating material formed as a flash. Suitable applications include the production of coated lightweight parts in areas where high corrosion resistance and wear protection are necessary.

2. Experimental setup and method

The modification of a milling machine (see Fig. 3) to serve as a friction surfacing machine allowed fast and easy coating of flat specimens. An inductor coil is used for heating up the coating material before and during the coating of the substrate. A pneumatic cylinder is used, pressing a carriage with the electric motor and the fixed coating rod against the substrate.

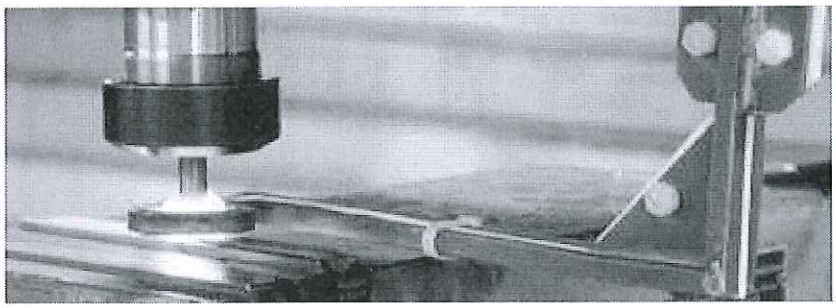

Fig. 3. Experimental setup: Modified milling machine.

2.1. Materials preparation

The parametric study was conducted by coating flat aluminium substrates (EN AW AlMgSi0,5 T66) of plate dimensions 20x6x135 mm, with stainless steel (X5CrNi18-

10) of consumable rod dimensions ∅10x96 mm. A separate *start plate* was manufactured out of mild steel (S235JR) showing dimensions 20x6x30 mm, as proposed by Chandrasekaran et al. (1997b). The substrate and coating material were prepared by an initial degreasing.

2.2. Machine concept and data acquisition

The friction surfacing machine had been optimized concerning repeatability by setting a mechanical stop to permit the coating rod to have a repeatable shortening of 50 mm during a given test. The shortening value was determined by preliminary trials showing the need to prevent the flash from contacting the collet chuck.

Measuring equipment was installed to ensure an accurate collection of data. The temperature of the coating rod at the contact zone (rod/substrate) was measured with a fixed pyrometer. The pyrometer employs an indium-gallium- arsenide-detector and operates at a shortwave length of 1.8 μm (shortwave infrared band). The device could be focused using its integrated laser beam, from a working distance of approximately 500 mm, to permit measurements from a zone of 2 mm in diameter. An emissivity of 0.8 was chosen for the stainless steel coating. A load cell is installed in between electric drive and pneumatic cylinder so as to monitor the process forces applied onto the drive and coating rod.

The coating material was preheated using an induction unit (5 kW output power) and then the coating process was started. Above 850 °C the ability of the inductive unit to increase the temperature of the coating rod significantly reduced; and so this defined the initial temperature. Meanwhile the inductive output power was maintained at a constant value.

After preheating the coating rod it was pressed onto the substrate, with an initial retention/dwell time of 12 seconds before the feed was started.

As the tests were made the mass, shortening and diameter of the flash of the coating rod was recorded. Machine parameters namely rotational speed (n [rpm]), pneumatic cylinder pressure (p [bar]) and travel speed (v [mm/min]) were documented. As this technique requires the initial use of a start plate, this sacrificial material must be cut away from the specimens so that the coating mass can be measured. The output param-

eters recorded were: the coating thickness (t [mm]), the coating mass (m_c or m [g]) and the consumption (s_B [mm]) as well as the consumption feed rate (v_B [mm/min]) of the coating rod. The coating thickness was measured along the coated layer, in the travel direction, at three points, employing a dial gauge (0-5 mm, +/-0.01 mm) allowing a mean value to be calculated. The coating mass was determined by weighing the substrate before and after the coating process; whereas the consumption feed rate could be calculated from the data produced by the inductive displacement transducer. This data is shown graphically in the Results section of this paper in a parameter by parameter basis. The tests have been repeated three times to gain higher statistical significance.

2.3. Bond strength and metallurgical investigation

The coating to substrate bond strength was determined by applying two concepts. On the one hand, the setup presented by Voutchkov et al. (2001) was employed to determine the push-off force necessary to completely fail the bond (Fig. 4). On the other hand, a shear test, as suggested by Khalid Rafi et al. (2010), was set up and is presented in Fig. 5.

The coated samples were cut into three parts (along the length of the specimens travel direction) to produce specimens for the push-off test, the shear test and a metallurgical investigation. The push-off test sample was cut from the first third of the coating, the shear test was cut from the last third; whilst the sample for the metallurgical investigations was taken from the middle part of the coated layer. It is noted that this method of selection may influence the test results if the coating process has not reached a stable state along the coated length. Consequently, push-off and shear test were additionally performed along the length of a given specimen and were found to be consistent.

Specimen preparation for the push-off test (see Fig. 4a) was completed by turning the coating to a cylindric form with a defined diameter as presented in Fig. 4bi. The diameter of this cylinder varies from 6 to 9 mm which was dependent on the coating width. The bore, cut through the thickness of the substrate so as not to penetrate the coating (see Fig. 4bii, was manufactured with either a diameter of 2 or 4 mm dependent on the substrate cylinder diameter used; an appropriate size push-off pin was then

inserted. During drilling it was checked that the bore was deep enough to just penetrate the coating-substrate interface. It is important to ensure that the area to be stressed does not include larger material bonding defects at the outside edge so as to prevent the occurrence of a notch effect (stress raiser). The setup was installed in an universal tensile testing machine and the applied force was increased until the bond failed (see Fig. 4biii.

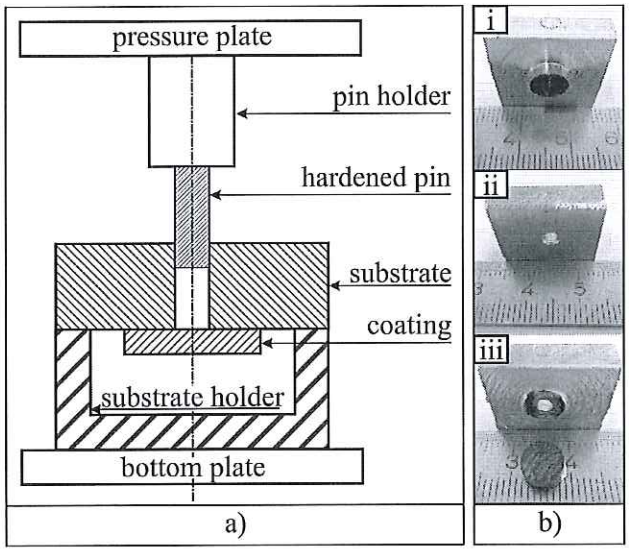

Fig. 4. a) Schematic drawing of the setup for tensile testing machine. b) Machined push-off specimen with turned stainless steel pin: i) prepared coating front view, ii) bore back view and iii) pushed off coating front view.

The shear test (see Fig. 5a) specimens were prepared by milling the coating whilst attached to the substrate to a length of 8 mm as shown in Fig. 5b. After inserting the specimen into a linear guide, the coating can be sheared off by increasing the applied force in the universal tensile test machine setup as shown in Fig. 5a. The test measured the maximum shear force carried by the coating-substrate bond.

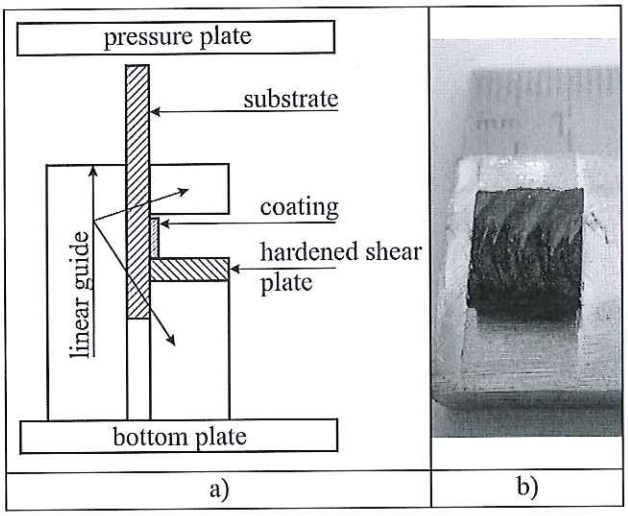

Fig. 5. a) Schematic drawing of the setup for tensile testing machine. b) Machined shear specimen with milled stainless steel coating.

The values for the bonded areas, were determined after the destructive push-off and shear tests with the accuracy afforded by using a calibrated image recognition tool as shown Fig. 6. The bond strength could then be determined.

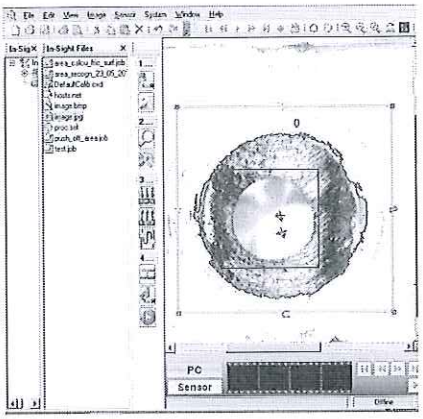

Fig. 6. Determination of the stressed push-off area with image recognition software.

3. Results

Fig. 7 presents data measured during the coating process against time. The induction preheating time of the stainless steel rod was approximately 135 seconds and the dwell time was set to a constant value of 12 seconds. The net coating time of about 35 seconds could be determined from the point when the feed of the coating rod along the substrate was started until the time when the process was stopped. Consequently the rod consumption s_B reduced to zero.

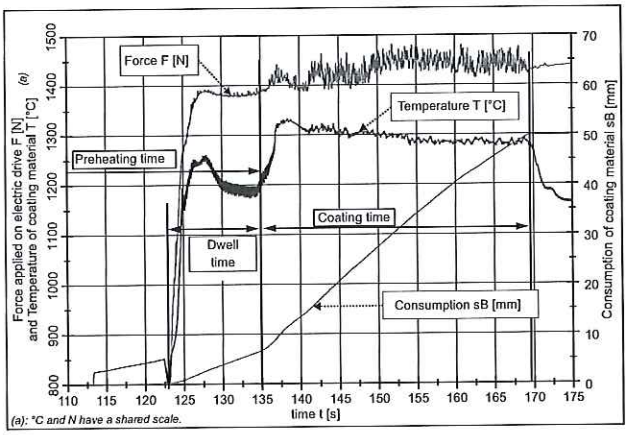

Fig. 7. Friction surfacing process graph: temperature of coating rod (the numeric scale for F and T are conveniently the same); force, due to pneumatic cylinder pressure, applied on coating rod via electric drive; and consumption of coating rod.

3.1. Coating geometry and mass

Fig. 8 through Fig.14 are presented to show relationships between various parameters which may be considered as 'output' and 'input' parameters. Output parameters consisted of coated mass (m_C), coating thickness (t) and consumption feed rate (v_B). The input parameters are consumable rod rotational speed (n) and pressure (p) with a constant travel speed of 150 mm/min.

The coated mass decreases by about 20 % for a doubling of the rotational speed with every pressure value (see Fig. 8), whilst the coating thickness generally decreases with increasing rotational speed (seeFig. 9). Now, Fig. 10a shows the resulting wedge shaped cross section of the stainless steel coating. Because of this form the coating

thickness varies within a given cross sectional slice. An additionally difficulty arises due to the slight distortion of the aluminium substrate (seeFig. 10b which produced an uneven contact on the measuring table.

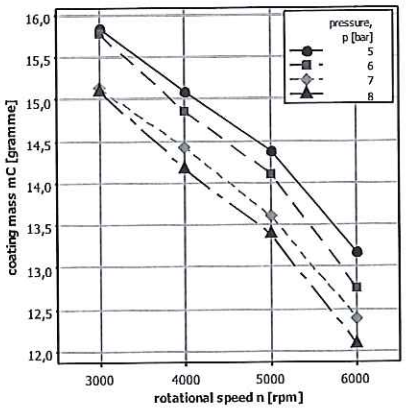

Fig. 8. The effect of rotational speed (n) on the coating mass (m), constant pressure (p) from 5 to 8 bar.

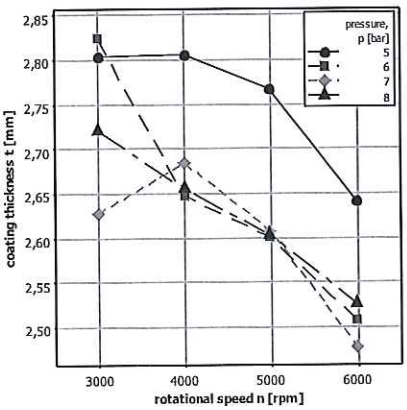

Fig. 9. The effect of rotational speed (n) on the coating thickness (t), constant pressure (p) from 5 to 8 bar.

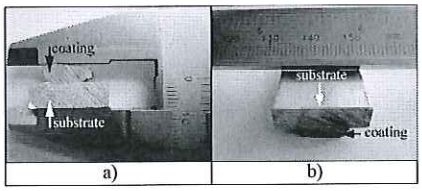

Fig. 10. a) Wedge shape of the stainless steel coating. b) Distortion of aluminium substrate.

It can be seen in Fig. 11 the consumption feed rate of the coating rod decreases with increasing rotational speed. The maximum feed rate is around 93 mm/min at maximum pressure and minimum rotational speed, which is reduced by about a third to a minimum value of 63 mm/min by doubling the rotational speed at minimum pressure.

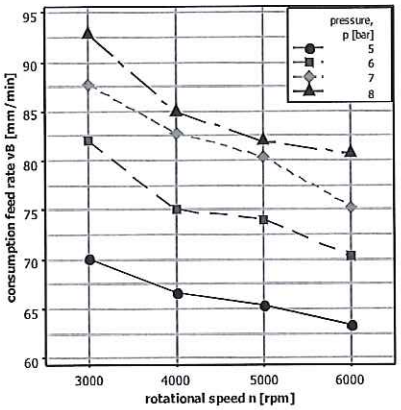

Fig. 11. The effect of rotational speed (n) on the consumption feed rate (v_B), constant pressure (p) from 5 to 8 bar.

The determination of the flash mass is calculated firstly by evaluating the consumed volume (of the coating rod), V, in the process which is:

$$V = a \cdot d^2 \cdot \pi \cdot 0.25 \tag{1}$$

where a is the burn-off length, which equates to the shortening of the coating rod, and d is the diameter of the coating rod (see Fig. 12). The volume of the coating (V_c) is:

$$V_c = m_c/\rho \tag{2}$$

where m_c is the mass of the coating and ρ is the density of the coating material. The volume of the flash is determined by the subtraction of the previously calculated volumes, namely:

$$\begin{aligned} V_F &= V - V_c \\ &= a \cdot d^2 \cdot \pi \cdot 0.25 - m_c/\rho \end{aligned} \tag{3}$$

The flash mass may be calculated by

$$\begin{aligned} m_F &= V_F \cdot \rho \\ &= a \cdot d^2 \cdot \pi \cdot 0.25 \cdot \rho - m_c \end{aligned} \tag{4}$$

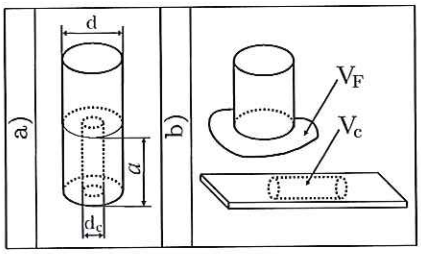

Fig. 12. Shortening of the coating rod (a) with diameter of real rotational contact plane (d_c, as defined by K Fukakusa (1996)): a) before and b) after the friction surfacing process.

According to Fig. 13, produced flash mass per coating mass increases with an increase in rotational speed. The flash mass is calculated by Equation 4. At 3000 rpm the flash mass created is about equal to the coating mass produced whilst at 6000 rpm and 8 bar cylinder pressure about three times as much flash is formed as coating material. If more material is produced as a flash at high rotational speeds, the coating mass per applied coating length decreases, as can be seen in Fig. 14.

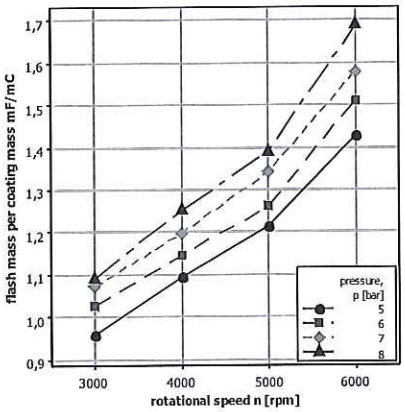

Fig. 13. The effect of rotational speed (n) on flash mass per coating mass, constant pressure (p) from 5 to 8 bar.

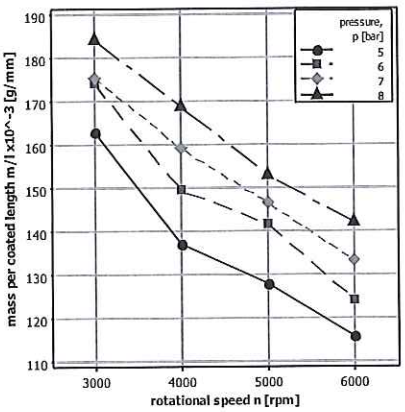

Fig. 14. The effect of rotational speed (n) on mass per coated length (m/l), constant pressure (p) from 5 to 8 bar.

3.2. Metallurgical aspects

Fig. 15a presents an SEM image of the interface between aluminium substrate and stainless steel coating where a flaw is evident within a groove. The observed cavity measures 134 μm in length and 55 μm wide. In some cases the groove is filled up completely with aluminium as is shown in Fig. 15b.

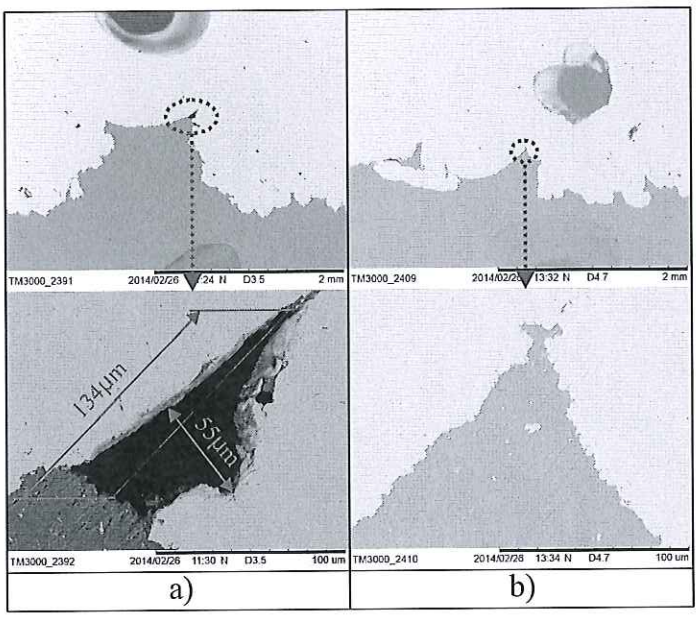

Fig. 15. a) SEM image of groove with cavitation (1000x). b) SEM image of groove completely filled with aluminium (1000x).

Fig. 16 shows a specimen where the coating (above) has been physically removed from the substrate (below). Mechanical deformation of the aluminium substrate created by the stainless steel coating results in regularly distributed grooves running transversely to the direction that the coating was formed. It can be clearly seen that the aluminium material is pressed into the grooves of the coating. Not every coating groove is completely filled with softened aluminium material and cavities may be created. This fact probably influences the push-off and shear strength values to a great extent.

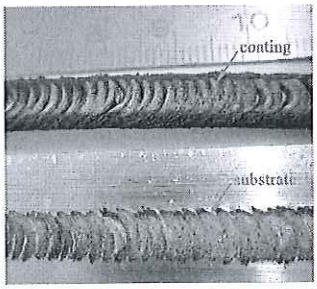

Fig. 16. Periodical produced caviations at bonding interface stainless steel on aluminium.

Fig. 17a) shows one specimen interface from a series of three repetitions. The grooves resulted in both a high push-off and a shear stress value of 107 MPa. Three grooves, up to a maximum 0.9 mm in depth and 2 mm in wide, are located on a cross section with a width of about 7.5 mm. Fig. 17b) shows another specimen interface, and when compared with Fig. 17a), shows very small grooves distributed along the cross section. In this second sample the degree of interlocking is low and showed a very poor push-off value of 15 MPa and a high shear stress value of 105 MPa. About 40 grooves may be observed which show a maximum of 0.1 mm in depth and 0.4 mm in width and which are located on the investigated width of 7.5 mm. The substantial amount of very fine mechanical interlocks may explain the high shear strength and relatively low push-off strength.

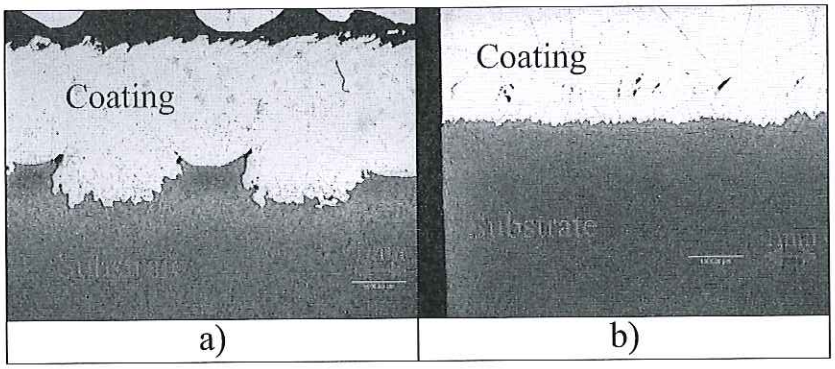

Fig. 17. a) High bond strength, parameters n=3000rpm and p=8bar, optical microscope, 50x. b) Low bond strength, parameters n=6000rpm and p=5bar, optical microscope, 50x.

3.3. Bond strength

A general decrease in the push-off strength with increasing rotational speed can be observed (Fig. 18). The highest strength with a mean of 96 MPa was obtained at 8 bar pressure and 3000 rpm. Standard error bars are calculated from performing three repetitions of each test showing a scattering of the values of up to 63 %.

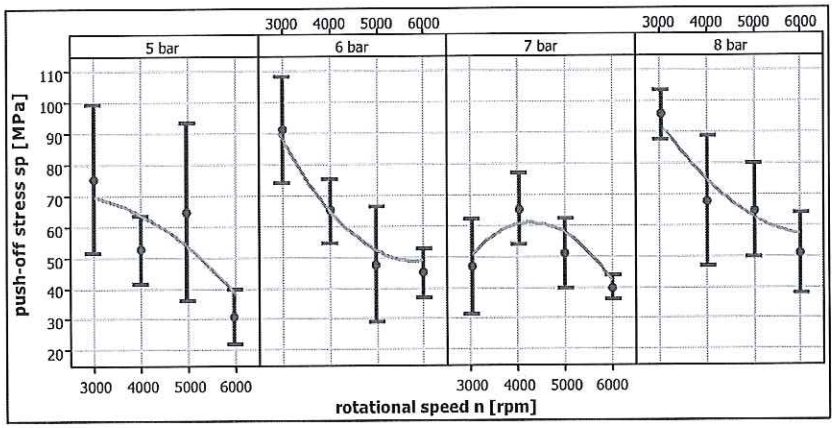

Fig. 18. The effect of rotational speed (n) on push-off stress (sp), for various pressure values (p) from 5 to 8 bar.

In contrast to the push-off values, Fig. 19 shows a marked increase in interfacial shear strength for lower coating rod pressure, at higher rotational speeds. This trend is not continued for the higher pressures which even show a decrease in bond strength for the highest rotational speeds. The maximum strength mean value of 106 MPa is attainable within a parameter frame of 5, 6 and 8 bar with rotational speeds of 4000, 5000 and 6000 rpm. Scattering of the values up to about 22 % is present.

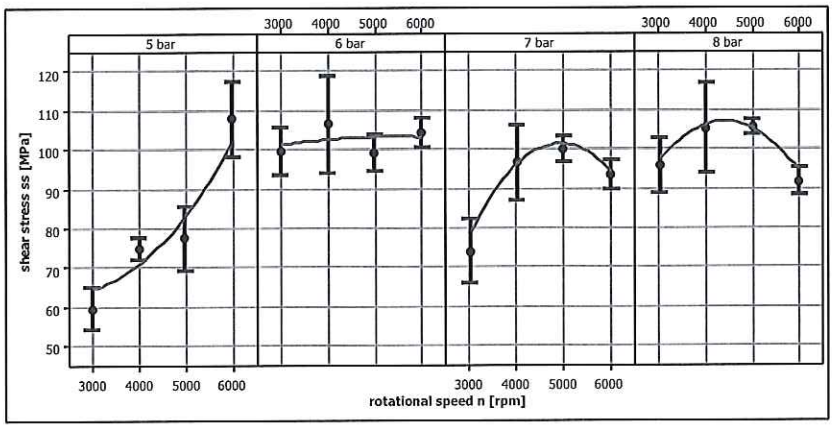

Fig. 19. The effect of rotational speed (n) on shear stress (τ), for various pressure values (p) from 5 to 8 bar.

The maximum coating bond strength values for both shear and push-off coatings exceed those of thermally sprayed X46Cr13 stainless steel coated on to low carbon steel: the values presented by Schiefler Filho et al. (2004) range in between 30 and 77 MPa. These values have been determined by employing the tensile test according to DIN EN 582 with cylinder specimens of 25 mm in diameter.

When investigating the edge of the coating (see Fig. 20a) a wedge shaped deformation of the aluminium substrate is evident. The hardened shear plate of the shear test setup (see Fig. 5a) has to be mounted in a such way so that this wedge is not contacted and additionally sheared off. The shear plate was mounted 2 mm from the substrate surface. Fig. 20b and c show that fracture occurred directly at the interface or within the aluminium substrate.

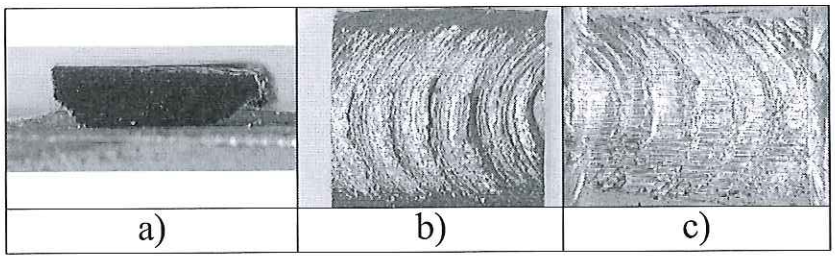

Fig. 20. a) Cross section of the aluminium deformation at the right and left edge of the coating. b) Sheared-off coating. c) Fractured surface of aluminium substrate.

Push-off specimens fractured either in a symmetric way or as presented in Fig. 21a where one edge adhered until the end of the test. Again, fracture occurred both directly at the interface and within the substrate (see Fig. 21b) and c).

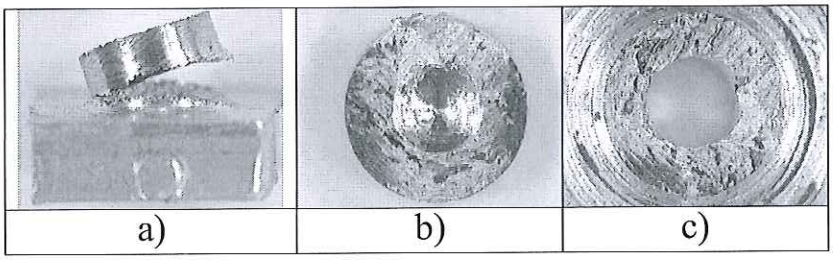

Fig. 21. a) Lifted coating. b) Pushed-off coating. c) Fractured surface of aluminium substrate.

4. Discussion

4.1. Principal parametric relationships

Coating mass, thickness and consumption feed rate of the coating rod were observed to demonstrate similar characteristics to that which has been reported in published work; albeit for other substrate-coating material combinations. The investigation of the flash volume produced shows that increasing pneumatic pressure and rotational speed results in an increasing flash volume. With an increasing rotational speed greater centrifugal forces may cause more material to be formed as a flash. On the other hand, the maximum coating mass per produced length could be determined at low rotation speed with high pneumatic cylinder pressure which results in the formation of a flash of an equal mass to that of the applied coating. There still is a need to reduce or eliminate the flash and an appropriate tool would improve the efficiency of the process. Decreasing trends of the push-off strength values for increasing rotational speeds may be due to the increase in flash volume which increases the contact area between rod and coating resulting in less surface pressure.

4.2. Bonding mechanism

The degree of mechanical interlocking resulting from the deformation of the substrate is clearly visible in various cross sectional slices and may be described as an 'interfacial roughness profile' which may be quantifiable. The reversal of trends demon-

strated by the push-off and shear bond strength values may be attributable to the difference in the interface roughness profile. The high interfacial roughness with only a few peaks and a high degree of substrate deformation, as presented in Fig. 17, results in good push-off values and relatively poor shear strength, whilst an increased amount of grooves with less depth result in good shear and poor push-off bond strengths (see Fig. 17b). The roughness peaks of up to 1 mm at the material interface limit the application to thicker substrates while the implementation of multiple passes of the coating rod needs further investigation for the production of larger coating areas.

Through the cross section randomly distributed cavitations are either present within the coating next to the interface or directly at the interface at the peaks of the mechanical interlocks. The latter influence the bond strength to a certain degree; cavitations have an detrimental effect on the reproducibility of a good bond.

The main bonding mechanism seems to be mechanical interlocking. However, some specimens show poor push-off strength values despite the presence of mechanical interlocks. This could be because of the presence of cavitations within the test specimens or because of poor surface adhesion in the mechanical interlocks. More research needs to be done to investigate the fractured specimen surface.

4.3. Fracture mode

Fracture during bond testing occurred as a mixed mode failure. Some of the aluminium material remained on the sheared or pushed-off coating while some fracture occurred at the interface probably contributing to the scattering of bond strength values. The heat input during the process, which resulted in interface temperatures above 1200°C, may result in artifical aging of the AlMgSi0.5 alloy. Production of $MgSi$ segregates and the presence of Al_2O_3 oxide inclusions of a size smaller than 1 μm might also contribute to the bond fracture properties. Further investigation would be necessary to detect such process products.

5. Conclusions

It is shown that stainless steel could be coated onto aluminium by additional inductive heating supplementing the heat produced by friction alone. Principal parametric relationships of input and output parameters were as follows:

(1) Coating mass and thickness decrease with increasing rotational speed and pneumatic cylinder pressure while the consumption feed rate of the coating rod decreases with increasing rotational speed and decreasing pneumatic cylinder pressure.

(2) The produced flash per coating mass is increased by 70 % by doubling the rotational speed resulting in less material per length being coated at the same time resulting in decreasing the process efficiency through increased material waste.

(3) The varying degree of mechanical interlocks and the presence of caviations at the coating-substrate interface result in a scattering of both shear and push-off bond strength values which show a decreasing trend for an increase in rotational speed.

(4) High bond strength values for both shear and push-off test could be obtained at 3000 rpm and 8 bar with a minimum amount of flash material being produced.

6. Acknowledgments

The authors would like to thank Werner Saft (Laboratory for Welding Techniques), Juergen Kotulla (Laboratory for Measuring Techniques) and Petra Schittenhelm (Laboratory for Material Sciences) at Kempten University of Applied Sciences for their support. The support of Nicola Kral is greatly appreciated.

7. References

Chandrasekaran, M., Batchelor, A., Jana, S., 1997a. Study of the interfacial phenomena during friction surfacing of aluminium with steels. Journal of Materials Science 32, 6055–6062.

Chandrasekaran, M., Batchelor, A.W., Sukumar, J., 1997b. Friction surfacing of metal coatings on steel and aluminum substrate. Journal of Materials Processing Technology 72, 446–452.

Gandra, J., Krohn, H., Miranda, R., Vilacca, P., Quintino, L., dos Santos, J., 2014. Friction surfacing—a review. Journal of Materials Processing Technology 214, 1062–1093.

Hanke, S., Beyer, M., Silvonen, A., dos Santos, J., Fischer, A., 2012. Cavitation erosion of Cr60Ni40 coatings generated by friction surfacing: article in press. Wear .

K Fukakusa, 1996. On the characteristics of the roational contact plane - a fundamental study of friction surfacing. Welding International 1996, 524–529.

Khalid Rafi, H., Janaki Ram, G., Phanikumar, G., Prasad Rao, K., 2010. Friction surfaced tool steel (H13) coatings on low carbon steel: A study on the effects of process parameters on coating characteristics and integrity. Surface and Coatings Technology 205, 232–242.

Lin, C.K., Berndt, C.C., 1994. Measurement and analysis of adhesion strength for thermally sprayed coatings. Journal of Thermal Spray Technology 3, 75–104.

Marot, G., Lesage, J., Démarécaux, P., Hadad, M., Siegmann, S., Staia, M., 2006. Interfacial indentation and shear tests to determine the adhesion of thermal spray coatings. Surface and Coatings Technology 201, 2080–2085. doi:10.1016/j.surfcoat.2006.04.046.

Schiefler Filho, M.F.O., Buschinell i, A.J.A., Gärtner, F., Kirsten, A., Voyer, J., Kreye, H., 2004. Influence of process parameters on the quality of thermally sprayed X46Cr13 stainless steel coatings. Journal of the Brazilian Society of Mechanical Sciences and Engineering 26, 98–106.

Stern, K.H., 1996. Metallurgical and ceramic protective coatings. 1st ed., Chapman & Hall, London and , New York.

Vitanov, V., Voutchkov, I., 2005. Process parameters selection for friction surfacing applications using intelligent decision support. Journal of Materials Processing Technology , 27–32.

Voutchkov, I., Jaworski, B., Vitanov, V.I., Bedford, G.M., 2001. An integrated approach to friction surfacing process optimisation. Surface and Coatings Technology , 26–33.